International Journal of Nanoelectronics and Materials
Volume 14, No. 4, October 2021 [399-408]

Studies on the Effect of MnO Doping on $LaFeO_3$ Ceramics in Comparison to Yarosite Mineral Properties for Ethanol Gas Sensors Performance

Endi Suhendi[1*], Latifah[1], Muhamad Taufik Ulhakim[1], Andhy Setiawan[1] and Dani Gustaman Syarif[2]

[1]*Program Studi Fisika, Universitas Pendidikan Indonesia, Bandung, Indonesia*
[2]*Pusat Sains dan Teknologi Nuklir Terapan, Badan Tenaga Nuklir Nasional, Bandung, Indonesia*

Received 14 April 2021, Revised 24 June 2021, Accepted 23 July 2021

ABSTRACT

This study aims to establish the effects of MnO doping in comparison on the yarosite mineral properties to determine its performance in the gas sensor applications. $LaFeO_3$ doped MnO was synthesized using coprecipitation method to be applied as ethanol gas sensors. The gas sensors were fabricated into thick ceramic film using screen printing techniques and analyzed using several characterizations such as XRD, SEM and electrical properties. The XRD data showed that the materials had a cubic structure and confirmed that the crystallite size had decreased from 49.83 nm to 43.20 nm. The SEM data showed that the materials had a grained morphology with the grain size of 0.61 µm and 0.36 µm, respectively. The electrical properties showed that the materials used had a sensitivity to ethanol gases; this was established from the resistances that appeared. It could be concluded that MnO doping caused the operating temperature of $LaFeO_3$ to become lower, decreasing from 272 °C to 268 °C. It was proven that the MnO (0.17 wt%) doping positively contributed to making the gas sensor's properties better. Thus, the yarosite mineral that contains 0.17 wt% of MnO as impurities can be applied as the main material in gas sensor studies.

Keywords: $LaFeO_3$, MnO, Yarosite Mineral, Thick Ceramic film, Ethanol Gas Sensors

1. INTRODUCTION

A gas sensor is an electronic device that produces electrical signals in response to the chemical interaction with gases [1]. One of the materials that can be used as a gas sensor is Metal Oxide Semiconductor (MOS) and it has been applied in the field of the solid-state sensing device, industrial fields, medical diagnostics and environmental monitoring [2]. $LaFeO_3$ is one of the metal oxide types which has an ABO_3 structure and can be used in various applications such as catalysts [3,4], electrodes [5], fuel cells [6] and gas sensors [7,8]. $LaFeO_3$ has good selectivity and a high response to gas sensors [9-11]. Ethanol gas sensors studies based on $LaFeO_3$ has been reported by Cao *et al.* to have the sensitivity of a gas sensor within the range between 30 to 50 with the operating temperature 110 °C to 135 °C [12-14]. However, $LaFeO_3$ has some disadvantages, which include a high resistance and it can be diminished with the additions of some dopant [15,16] as reported by Liu *et al.* [17], Sun *et al.* [18], Cyza, *et al.* [19], Koonsaeng, *et al.* [20] and Xiang, *et al.* [21]. The findings concluded that dopant has an essential effect on gas sensors performances. Their studies indicated that it had a sensitivity to the presence of ethanol gases. Most of the earliest studies were obtained using precursor Fe_2O_3 from pure materials.

Indonesia is one of the countries in the world that has abundant minerals resources and one of them that is widely available is yarosite mineral [22]. Yarosite mineral contains 91.30 wt% Fe_2O_3 and several other minerals, namely 3.30 wt% of Al_2O_3, 2.05 wt% of SiO_2, 3.02 wt% of

*Corresponding author: endis@upi.edu

TiO_2, 0.16 wt% of CaO and 0.17 wt% of MnO [23]. The aim of this study is to examine the MnO component of the yarosite minerals in order to determine the effect it has on the ethanol gas sensor. In this paper, we analyzed the effect of MnO doping on $LaFeO_3$ thick film ceramic and compared it with yarosite mineral properties in order to establish any differences in the performance of ethanol gas sensor. MnO is one of the oxide transition metals that has room temperature ferromagnetic properties and if MnO is inserted into $LaFeO_3$, it can improve the sensor's performance [24]. The composition of MnO doping added to this work is 0.17 wt%, which is based on the MnO composition of yarosite minerals. The crystal structure, morphology and electrical properties, including an operating temperature of thick film ceramic based on $LaFeO_3$ doped MnO, were analyzed. If MnO doping generated a good characteristic that can decrease an operating temperature and increase the sensitivity of gas sensors, MnO in yarosite mineral should not be removed in the Fe_2O_3 purification process. This will conclude whether Fe_2O_3 from the yarosite mineral can be applied as the main material of ethanol gas sensors.

2. EXPERIMENTAL DETAILS

In this work, $LaCl_3.7H_2O$ (2.013 g) and Fe_2O_3 (0.987 g) were used to make $LaFeO_3$ powders and $LaCl_3.7H_2O$ (2.323 g); Fe_2O_3 (0.952 g) and MnO (0.01 g) were used to make $LaFeO_3$ doped MnO powders. It was made using the coprecipitation method, as shown in Figure 1. All the materials are dissolved in the solvent using a magnetic stirrer where the Fe_2O_3 and MnO are dissolved in HCl while $LaCl_3.7H_2O$ is dissolved in aqua dest. Then, all the solutions are mixed using a magnetic stirrer and heated to 80 °C. The aim of the process is to make a homogeneous solution. After that, each solution is added to NH_4OH to precipitate the solution. The precipitate is dried at 100 °C and then calcined at 800 °C for 2 hours. After being calcined, the precipitate is ground and strained to produce uniform nano-sized powders.

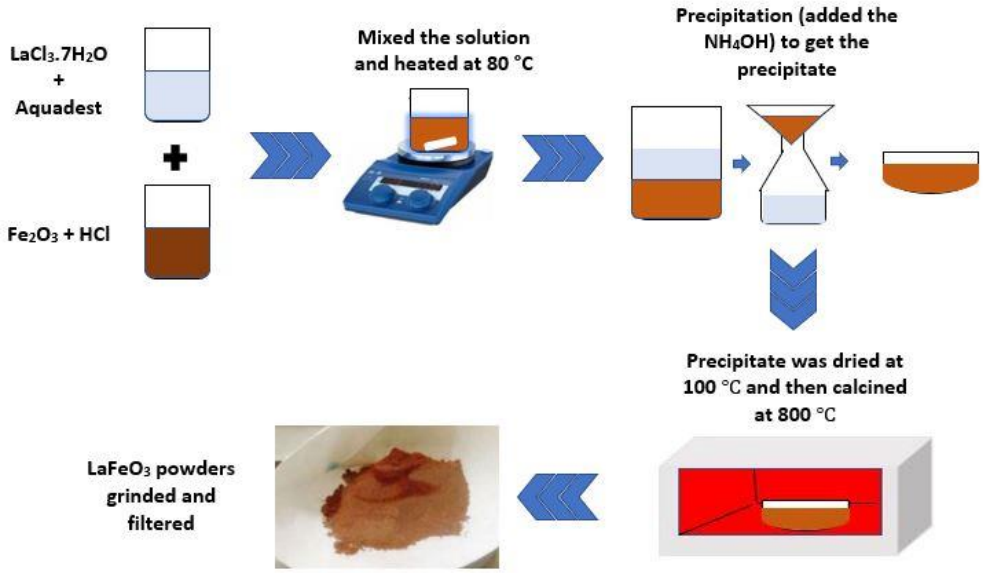

Figure 1. The synthesis process of $LaFeO_3$ powders

The same process is carried out to produce the $LaFeO_3$ doped MnO. The difference is the addition of the MnO solution when creating the mixed solution. $LaFeO_3$ and $LaFeO_3$ doped MnO powders are made in thick ceramic film, as shown in Figure 2. To make thick films, both material powders are mixed with Organic Vehicle (OV) in the ratio of 70 wt% and 30 wt%, so that the material powders will turn to a paste. The paste is then coated on an alumina substrate coated with silver using the screen-printing method and fired at 500 °C for 2 hours.

$LaFeO_3$ and $LaFeO_3$ doped MnO thick-filmed ceramics were characterized using X-Ray Diffraction (XRD) PRO Series λ = 1.540598 Å PAN to identify the crystal structure. A Scanning Electron Microscopy (SEM) JEOL-6360LA is used to identify the morphological structure and a set of gas chamber tools is used to establish the electrical properties, as shown in Figure 3.

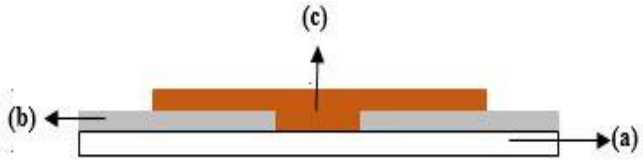

Figure 2. Illustration of thick ceramic film layers based $LaFeO_3$ and $LaFeO_3$ doped MnO: (a) alumina substrate (b) silver (c) materials paste

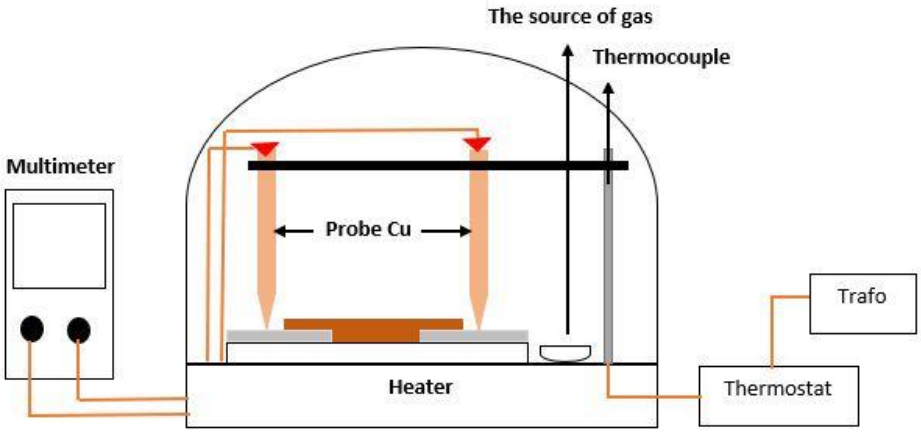

Figure 3. Illustration of gas chamber tools to recognize the electrical properties

The measurement of the electrical properties was done by heating the thick ceramic film from room temperature to 350 °C. During the measurement process, the resistance values were recorded at 2 °C temperature change. It was done on the ambient state (without gases) and with the addition of ethanol gases at a concentration of 100 ppm, 200 ppm, and 300 ppm.

2. RESULTS AND DISCUSSION

The result of the characterization of the crystal structure is presented in Figure 4. It is presented in the form of peaks that indicate the presence of the crystalline phases. These results were matched to the peak at the diffraction data standard COD (Crystallography Open Database) using Match 3 software. This characterization covers crystal structure, index miller values, lattice parameter and crystallite size. The referring data suggested that the formed crystal structure was cubic. It can be seen from the index miller values (hkl) of the data that each diffraction angle 2θ produces a peak, as shown in Table 1. The lattice parameter of $LaFeO_3$ and $LaFeO_3$ doped MnO are $a = b = c = 3.9361$ Å and $a = b = c = 3.9373$ Å, respectively and it shows that the lattice parameter of both thick ceramic film is not significantly different and it did not change the crystal structure. The average crystallite size was obtained using the Debye-Scherrer Equation as shown in Equation (1) [25]:

$$D = 0.89\lambda/B\cos\theta \quad (1)$$

where D is the average of crystallite size (nm), 0.89 is the Scherrer constant which has a value between the range 0.8 – 1.0 and 0.89 is assumed to be the best value in this present work, λ is the

wavelength of X-rays that used in this work (1.540598Å), B is the full width at half maximum (FWHM) and θ is the Bragg diffraction angle. The calculation found that the average crystallite size of $LaFeO_3$ and $LaFeO_3$ doped MnO are 49.83 nm and 43.20 nm, respectively. Based on these results, the addition of MnO doping can reduce the crystallite size and it means that La^{3+} has been successfully substituted by Mn^{2+} in $LaFeO_3$. It also informs that the MnO containing yarosite mineral provides a positive contribution to the crystal structures.

The result of morphological structure characterization is shown in Figure 5. The differences are observed in the morphological scale and it looks like the grain size of $LaFeO_3$ thick film ceramic is larger than the $LaFeO_3$ doped MnO thick film ceramic. They are 0.61 μm and 0.36 μm, respectively. MnO doping can reduce the grain size. It may cause MnO doping to hinder the movement of the grain boundaries once it serves as a deterrent to irregular grain growth. The sensitivity will be sharply increased if the grain size is decreased. It was similar to the claims made by Xiaoshui [3]. The decreasing grain size when MnO is added to $LaFeO_3$ will make the sensitivity of $LaFeO_3$ doped with MnO increase higher than the $LaFeO_3$ sensitivity.

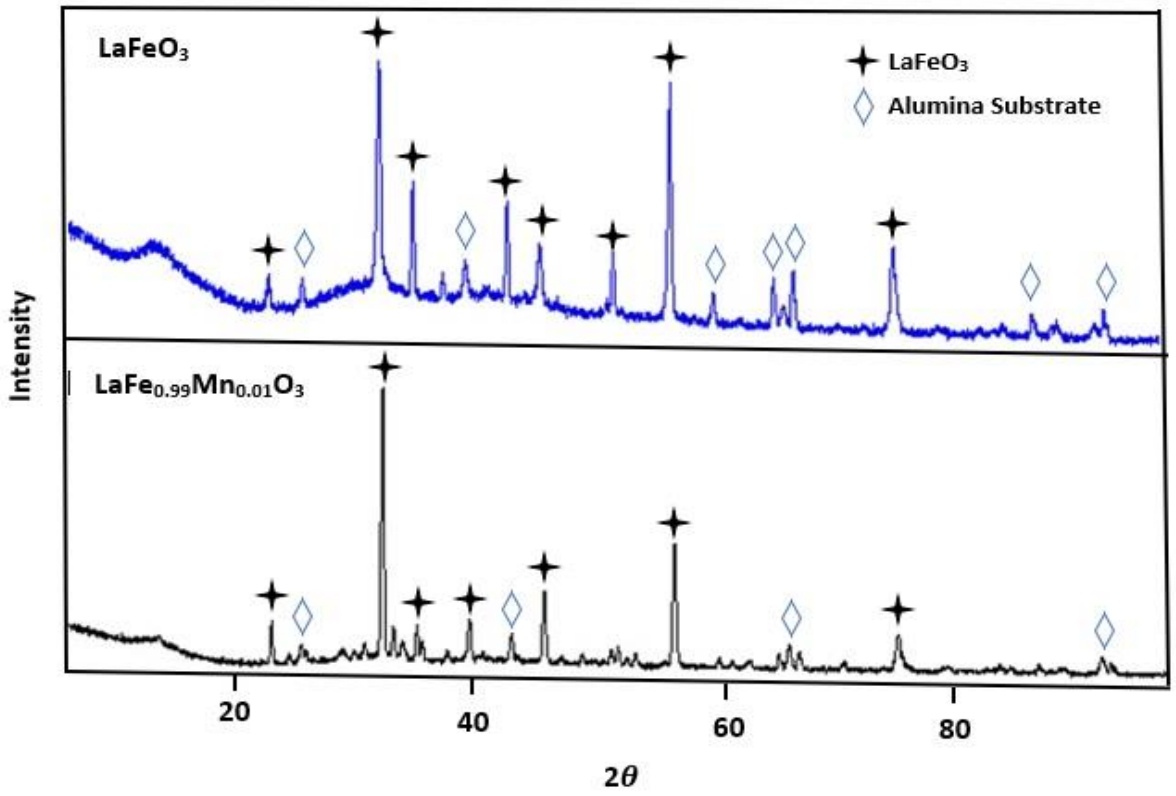

Figure 4. Pattern of (a) $LaFeO_3$ (b) MnO doped $LaFeO_3$

Table 1. Index miller values (hkl)

No.	**LaFeO3**		**$LaFe_{0.99}Mn_{0.01}O_3$**	
	Crystallite Size: **49.83 nm**		**43.20 nm**	
	2θ	hkl	2θ	hkl
1	22.47	100	22.38	100
2	32.08	110	32.06	110
3	39.60	111	39.57	111
4	46.07	200	46.05	200
5	57.34	211	51.90	210
6	67.28	220	57.36	211

7	71.99	221	67.25	220
8	76.63	310	76.75	310
9	85.50	222	94.29	321
10	94.29	321	-	-

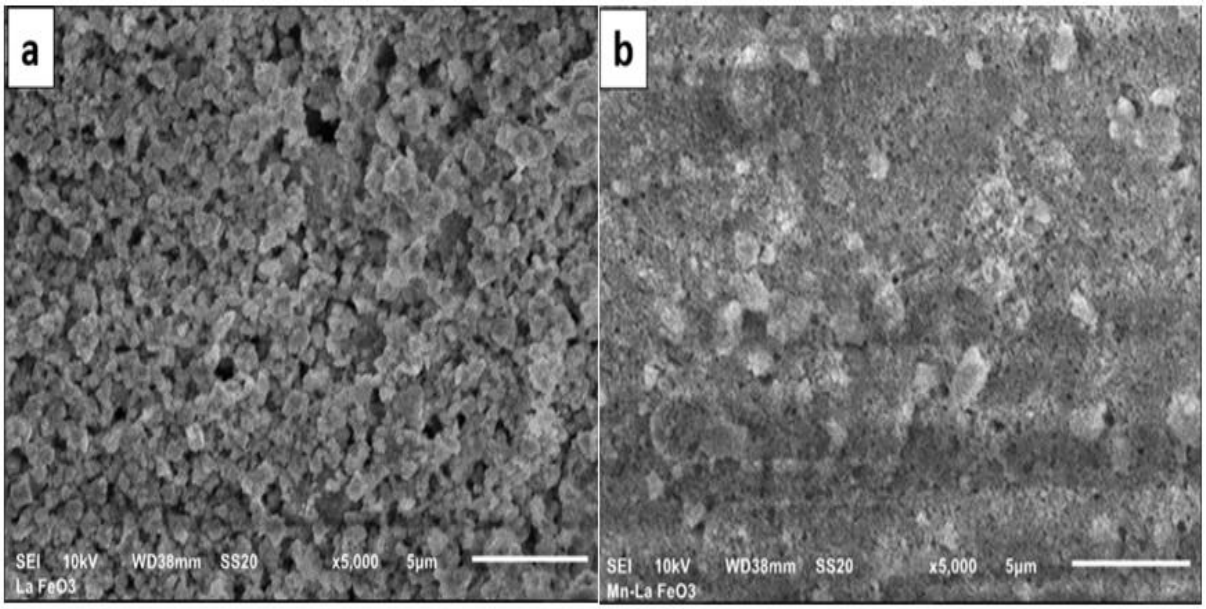

Figure 5. Morphology structure of (a) $LaFeO_3$ (b) MnO doped $LaFeO_3$

Electrical properties characteristics of $LaFeO_3$ thick film ceramic without doping and with MnO doping can be seen in Figure 6. Figure 6 presents the graph of resistance to temperature. Apart from that, it shows that the resistance of thick films has decreased exponentially when the temperature is increased, which is one of the characteristics of semiconductor [26]. It is caused by a number of electrons in the valence band excited reaction to the conduction band. In the higher temperature, more electrons would be excited. The electrons that have been excited to the conduction band will be the delocalized electrons. It is easier for the thick ceramic film to conduct the electric current if more electrons move to the conduction band and the resistance values are smaller.

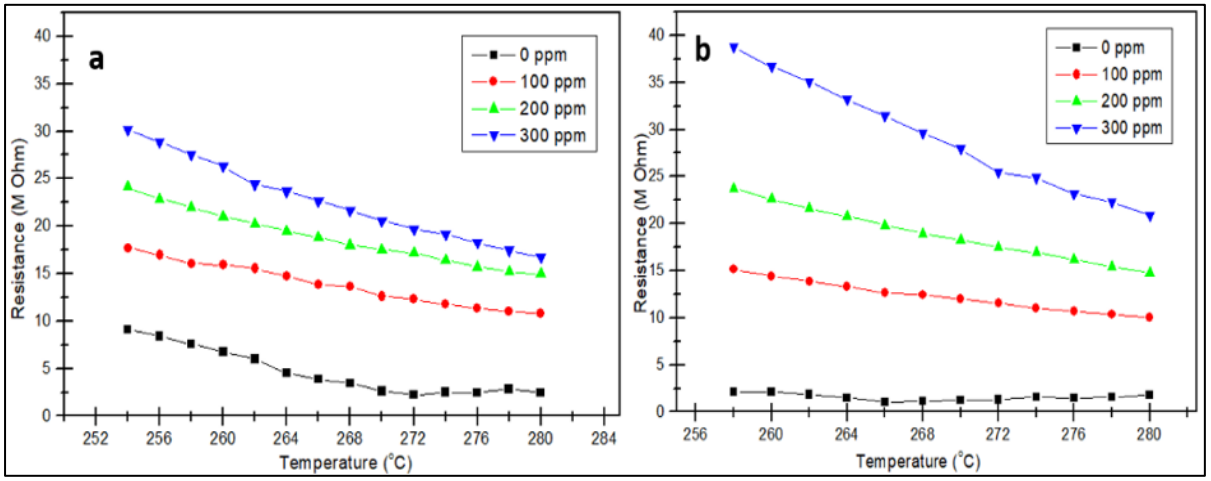

Figure 6. The graph of resistance to the temperature of (a) $LaFeO_3$ (b) MnO doped $LaFeO_3$

The resistance increases with the increasing ethanol gas concentration at the same temperature, as shown in Figure 6. It causes the ethanol gas to be the reducing gas and this indicates that the semiconductor is p-type, which has the charge of the majority carriers in the form of holes. The p-type semiconductor will decrease the conductivity value (major resistance) when it interacts with the reducing gases [27].

Sensitivity is the response of the material to gas indicated by a change in resistance due to gas absorption in accordance with Equation (2) [28]:

$$S = (R_e\text{-}R_o)/R_o \quad (2)$$

where S is the sensitivity of the gas sensor based on the thick film, R_e is the resistance of the gas sensor based on the thick film in the gas chamber containing ethanol gas and R_o is the resistance of the gas sensor based on the thick film in the gas chamber without ethanol gases. Thus, sensitivity according to Equation (2) is a comparison of the difference in the resistance of the gas sensor before and after the presence of ethanol gas and the resistance before the presence of ethanol gas.

The graph of temperature sensitivity is shown in Figure 7. It can be seen that the operating temperature of $LaFeO_3$ thick film ceramic without doping and $LaFeO_3$ thick film ceramic with MnO doping are 272°C and 268°C, respectively.

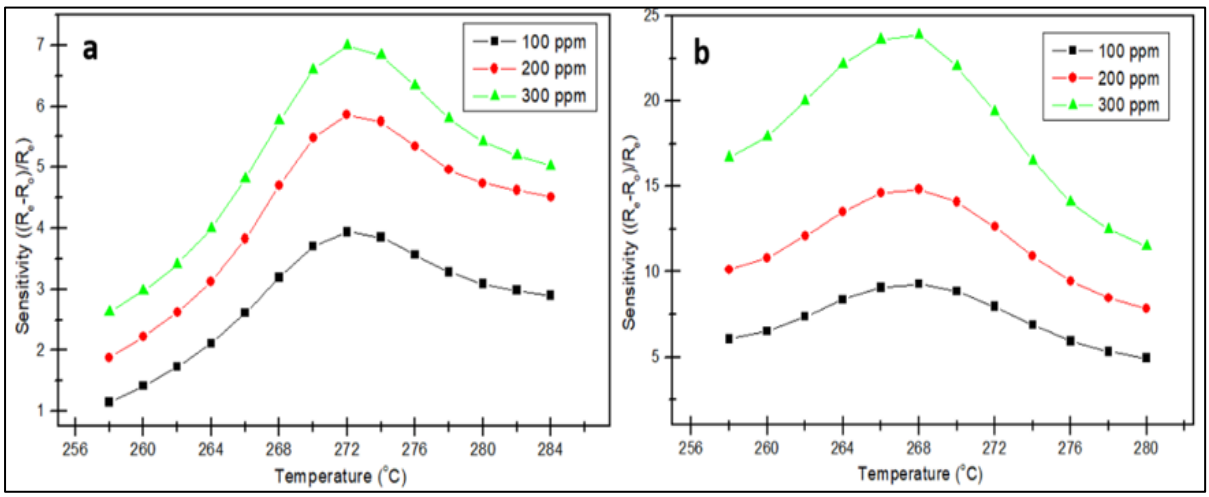

Figure 7. Graph of sensitivity to temperature of thick film ceramic based on (a) $LaFeO_3$ (b) MnO doped $LaFeO_3$

The sensitivity will be greater when the gas concentration is higher. It happens because when the gas sensor based on the thick film ceramic is heated in the ambient condition (absence of ethanol gases), the surface of the thick film will absorb the O_2 gases and it will create a reaction on the surface of the thick film. The reaction will change the O_2 gases to O^- or O^{2-} ion. One of the ions will become more dominant, which is caused by the type of material employed and the presence of reducing gas. When the thick film ceramic is in an environment and it consists of gas molecules of ethanol, the ethanol gas molecules will react with oxygen gas molecules that have been ionized (O^- and O^{2-}) to form CO and H_2O [27,29]. As a p-type semiconductor material, the population of holes is greater than the electron. Thus, the holes attract new electron and become annihilated. The number of charge carriers (holes) in the valence band will be reduced resulting in the increase in electric resistance, as shown by the increase of activation energy in Table 2. The activation energy is calculated using Arrhenius relation as shown in Equation (3) [30]:

$$\sigma = \sigma_0 \exp(-E_a/kT) \quad (3)$$

where σ_0 is the frequency factor, E_a is the activation energy, k is the Boltzmann constant and T is the absolute temperature in kelvin (K) [31, 32]. If the activation energy is high, the sensitivity will

increase. For the undoped sensors, activation energy is needed to adsorb oxygen and ethanol reaction because of the optimal temperature of a high doped sensor. As for doped sensors, a low activation energy value can provide a reaction pathway. Therefore, the sensor can provide a maximum response at low temperatures [33].

Table 2. Energy Gap of thick films ceramics

Doping MnO (wt%)	Ethanol Gas concentration (ppm)	Activation energy (eV)	Sensitivity
0	0	0.69	-
	100	0.92	3.94
	200	0.93	5.86
	300	1.12	6.98
0.17	0	0.15	-
	100	0.87	9.28
	200	1.01	14.83
	300	1.38	23.89

3. CONCLUSIONS

$LaFeO_3$ doped by MnO is successfully prepared using the coprecipitation method and is then compared to yarosite mineral properties to determine its effectiveness on ethanol gas sensor performances in the form of thick ceramics film. In this research, the thick ceramics films are made using screen printing techniques. Based on the findings, it is established that the material has a cubic structure with crystallite sized 49.83 nm and 43.20 nm and the grain size of 0.61 μm and 0.36 μm, respectively. Apart from that, this study also establishes that the ethanol gas sensor made possesses a greater sensitivity and lower operating temperatures; it is 272 °C for $LaFeO_3$ and 268 °C for $LaFeO_3$ doped MnO. It can be concluded that MnO doping has an effect on gas sensor performance, such as decreasing the size of the crystallite, the grain size and the operating temperature. It can be concluded that MnO doping has a positive contribution and should not be removed in the purification process of yarosite minerals. It means that the yarosite mineral that contains 0.17 wt% MnO as impurities can be applied as a main material in gas sensor studies.

ACKNOWLEDGEMENT

This work was financially supported by the "Hibah Penelitian Terapan Unggulan Perguruan Tinggi" Kementerian Riset, Teknologi dan Pendidikan Tinggi Republik Indonesia Research Grants in the fiscal year 2019.

REFERENCES

[1] A. K. Yadav, R. K. Singh, P. Singh. Sens. Actuators B Chem. (2016) 229, 25-30.
[2] K. P. Priyanka, S. C. Vattappalam, S. Sankararaman, K. M. Balakrishna, T. Varghese. Eur. Phys. J. Plus. (2017) 132, 306.
[3] X. Zhang, R. Gu, J. Zhao, G. Jin, M. Zhao, Y. Xue. J. Mater. Eng. Perform. 24, 3815-3819 (2015).
[4] H. Zhu, P. Zhang, S. Dai. ACS Catal. (2015) 5, 6370-6385.
[5] J. W. Yoon, M. L. Grili, E. D. Bartolomeo, R. Polini, E. Traversa. Sens. Actuators B Chem. (2001) 76, 483-488.
[6] T. Hong, F. Chen, C. Xia. J. Pow. Sour. 278, 741-750 (2015).
[7] J. Qin, Z. Cui, X. Yang, S. Zhu, Z. Li, Y. Liang. Sens. Actuator B Chem. (2015) 209, 706-713.

[8] Y. M. Zhang, Y. T. Lin, J. Zhang, Z. Q. Zhu, Q. Liu, Q. J. Liu. App. Mech. Mater. (2013) 320, 554-557.
[9] J. Zhang, Y. M. Zhang, C. Y. Hu, Z. Q. Zhu, Q. J. Liu. Adv. Mater. Res. (2013) 873, 304-310.
[10] T. F. Du, Y. M. Zhang, J. Zhang, Z. Q. Zhu, Q. J. Liu. Mater. Sci. Forum. (2016) 852, 760-765.
[11] W. Wei, S. Guo, C. Chen, L. Sun, Y. Chen, W. Guo, S. Ruan. J. Alloy Compd. (2017) 695, 1122-1127.
[12] E. Cao, H. Wang, X. Wang, Y. Yang, W. Hao, L. Sun, Y. Zhang. Sens. Actuators B Chem. (2017) 251, 885-893.
[13] E. Cao, Y. Yang, T. Cui, Y. Zhang, W. Hao, L. Sun, H. Peng, X. Deng. App. Surf. Sci. (2017) 393, 134-143.
[14] E. Cao, Z. Chu, H. Wang, W. Hao, L. Sun, Y. Zhang. Ceram. Int. (2018) 44, 7180-7185.
[15] C. Doroftei, P. D. Popa, F. Iacomi. Sens. Actuators A Phys. (2013) 190, 176-180.
[16] A. Benali, S. Azizi, M. Bejar, E. Dahri, M. F. P. Garaca. Ceram. Int. (2014) 40, 14367-14373.
[17] X. Liu, B. Cheng, J. Hu, H. Qin, M. Jiang. Sens. Actuator B Chem. (2008) 129, 53-58.
[18] L. Sun, H. Qin, K. Wang, M. Zhao, J. Hu. Mater. Chem. Phys. (2011) 125, 305-308.
[19] A. Cyza, A. Kopia, L. Cieniek, J. Kusinski. Mater. Today Proc. (2016) 3, 2707-2712.
[20] N. Koonsaeng, T. Thaweechai, A. Wisitsoraat, W. Wattanathana, S. Wannapaiboon, S. Chotiwan, C. Veranitisagul. A. Laobuthee. SOJ Mater. Sci. Eng. (2018) 6, 1-9.
[21] J. Xiang, X. Chen, X. Zhang, L. Gong, Y. Zhang, K. Zhang. Mater. Chem. Phys. (2018) 213, 122-129.
[22] H. Aliah, D. G. Syarif, R. N. Iman, A. Sawitri, M. Sanjaya, M. N. Subkhi, P. Pitriana. IOP Conf. Ser.: Mater. Sci. Eng. (2018) 367, 012041.
[23] N. I. Ariyani, D. G. Syarif. E. Suhendi. IOP Conf. Ser.: Mater. Sci. Eng. (2018) 384, 012037.
[24] R. S. Ganesh, E. Durgadevi, M. Navaneethan, V. L. Patil, S. Ponnusamy, C. Muthamizhchelvan, S. Kawasaki, P. S. Patil, Y. Hayakawa. J. Alloy Compd. (2017) 721, 182-190.
[25] Q. Zhou, A. Umar, E. M. Sodki, A. Amine, L. Xu, Y. Gui, A. A. Ibrahim, R. Kumar, S. Baskoutas. Sens. Actuators B Chem. (2017) 259, 604-615.
[26] R. Godbole, V. P. Godbole, P. S. Alegaonkar, S. Bhagwat. New J. Chem. (2017) 41, 11807-11816.
[27] G. F. Fine, L. M. Cavanagh, A. Afonja, R. Binions. Sensors. (2010) 10, 5469-5502.
[28] E. Suhendi, H. Novia, D. G. Syarif. Conference: International Conference on Mathematics and Natural Sciences. (2010) 600-607.
[29] W. Haron, A. Wisitsoraat, S. Wongnawa. Ceram. Int. (2017) 43, 5032-5040.
[30] C. Balamurugan, D. W. Lee. Sens. Actuators B Chem. (2015) 221, 857-866.
[31] T. Kurniawan, F. A. B. Fauzi, Y. P. Asmara. Indonesian J. Sci. Tech. (2016) 1, 107-114.
[32] A. M. Anshar, P. Taba, I. Raya. Indonesian J. Sci. Tech. (2016) 1, 47-60.
[33] G. Singh, M. Kaur, B. Arora, R. C. Singh. J. Mater. Sci.: Mater. Electron. (2018) 29, 867-875.